DOI: 10.2352/ISSN.2470-1173.2016.18.DPMI-252

A Three Parameter Underwater Image Formation Model

Henryk Blasinski, Department of Electrical Engineering, Stanford University, Stanford CA
Joyce Farrell, Department of Electrical Engineering, Stanford University, Stanford CA

Abstract

We developed an underwater image formation model that describes how light is absorbed and scattered by seawater and its constituents. We use the model to predict digital camera images of a reference target with known spectral reflectance at different distances and depths. We describe an inverse estimation method to derive three model parameters: phytoplankton absorption spectrum, chlorophyll concentration and the amount of colored dissolved organic matter or CDOM. The estimated parameters predict the spectral attenuation of light which can be used to color balance the images. In addition, parameter estimates can be used to monitor environmental changes turning a consumer digital camera into a scientific measurement device.

Introduction

The digital camera has become an accessory that most people take with them everywhere, including underwater. Sadly, they are often disappointed with the quality of their underwater images. Backscattered light reduces image contrast and wavelength dependent light absorption by water introduces color changes [1, 2]. No doubt the quality of underwater photography will improve as the low-light sensitivity of imaging sensors increases and as new image processing methods are introduced.

Several underwater image correction algorithms operating on RGB images have been proposed [3, 4], but only a few methods analyze the data in the spectral wavelength domain [5, 6, 7]. In most cases, the goal of these algorithms is to improve color rendering, rather than infer biologically relevant quantities [7, 8, 9]. In this paper we consider how to derive scientific data from underwater camera sensor images in order to characterize the ocean seawater environment. We also illustrate how this data can be used to process and improve the perceived quality of underwater images.

We developed an underwater image formation model to describe how light is absorbed and scattered by water and its constituents and how light is captured by the imaging sensor in a digital camera. We use our model to simulate the appearance of images captured by digital cameras and to relate the appearance to physically interpretable quantities, such as the type and amount of phytoplankton and other organic and inorganic matter in sea water [10]. We also use the insights we gained from these simulations to improve the way we process underwater images in order to produce more aesthetically pleasing photographs [7].

Our underwater image formation model is composed of three components. First, we use the underwater image formation model of Jaffe and McGlamery [11, 12] to describe light absorption and scattering in units of medium beam absorption and scattering coefficients. Second, we incorporate the results of oceanographic and biological research describing attenuation and scattering coefficients as functions of concentrations of fundamental constituents of sea water: phytoplankton, colored dissolved organic matter (CDOM) and non-algal particles (NAP) [10]. Third, we use a full camera simulation package (ISET, [13]) to produce simulated images of underwater targets.

We use the underwater image formation model to predict the sensor data captured by a digital camera at a fixed distance and depth from a reference target with known spectral reflectance. With the appropriate parameter settings, we can reproduce the appearance of sensor images captured by real cameras in similar underwater environments.

We wish to use the digital camera as a scientific instrument that can measure environmental factors, such as the type and concentration of phytoplankton and other material in the seawater. To accomplish this, we introduce an inverse estimation method that uses the camera sensor data to derive parameters that describe 1) the spectral absorption of light by phytoplankton, 2) the concentration of chlorophyll in phytoplankton, and 3) the amount of colored dissolved organic matter or CDOM.

We use the inverse estimation method as a metric to evaluate how well any digital camera can be used to measure environmental parameters and consider how these measurements can also be used to improve the perceived quality of underwater images.

Image formation model

The measurement m produced by an imaging device is linearly related to device's spectral sensitivity functions $p(\lambda)$ and the light radiance $\rho(\lambda)$ reaching the photodetector [14]

$$m = \int p(\lambda)\rho(\lambda)d\lambda. \tag{1}$$

A ray of light traveling between the source and the scene interacts with the medium in two ways. First, some of the light may be absorbed by the medium, and thus the overall intensity of light is reduced. Second, the direction of propagation of a portion of the light ray may be changed in a phenomenon called scattering. As a consequence of these interactions the total radiance along a particular ray of light $\rho(\lambda)$ reaching an imaging device can be decomposed into two additive components; direct $\rho_d(\lambda)$ and backscattered $\rho_b(\lambda)$ [1, 11, 12]

$$\rho(\lambda) = \rho_d(\lambda) + \rho_b(\lambda). \tag{2}$$

The direct component contains all the light rays that, having been emitted by a source, interact with a scene. The backscattered component represents all the light rays whose direction of propagation was changed by the medium before they reached the target, which means they are captured by the imaging device without interacting with the scene (Fig. 1).

The McGlamery-Jaffe underwater image formation model [11, 12] describes how the absorption and scattering affect the

DOI: 10.2352/ISSN.2470-1173.2016.18.DPMI-252

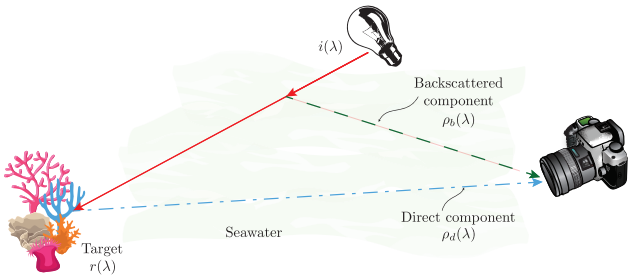

Figure 1: Direct and backscattered components in underwater imaging.

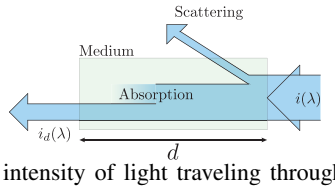

Figure 2: The intensity of light traveling through a medium is reduced due to absorption and scattering.

direct and backscattered radiance components. However, for uniform surfaces at a fixed distance from the camera the radiance of the direct component depends on the light source spectral power distribution $i(\lambda)$, target surface spectral reflectance $r(\lambda)$, and the attenuation of light introduced by the medium $c(\lambda)$. The relationship is governed by the Beer-Lambert attenuation law [7]

$$\rho_d(\lambda) = r(\lambda)i(\lambda)e^{-dc(\lambda)}, \tag{3}$$

where d is the distance light travels through the medium.

Total attenuation coefficient

The total attenuation coefficient $c(\lambda)$ describes how much light at wavelength λ is attenuated as it travels through the medium. Light attenuation depends on how much the medium absorbs light as well as how much light is scattered. The contributions of these two phenomena, denoted $a(\lambda)$ and $b(\lambda)$ for absorption and scattering respectively, define the total absorption coefficient $c(\lambda)$

$$c(\lambda) = a(\lambda) + b(\lambda). \tag{4}$$

Intuitively, the intensity of a particular ray of light traveling through a medium can be decreased either because photons are absorbed by the medium, or because some of the light starts to propagate in different direction as it is reflected off small particles suspended in that medium. Along the ray however the net effect of these two distinct phenomena is the same; light intensity is reduced (Fig. 2).

Absorption coefficient

In underwater environments, the absorption coefficient is impacted by the optical properties of pure sea water $a_w(\lambda)$ and the absorption properties of three seawater constituent particles: phytoplankton $a_\Phi(\lambda)$, colored dissolved organic matter (CDOM), $a_{\text{CDOM}}(\lambda)$, and non-algal particles (NAP), $a_{\text{NAP}}(\lambda)$. The total absorption coefficient is given by the sum of absorption properties of the constituents

$$a(\lambda) = a_w(\lambda) + a_\Phi(\lambda) + a_{\text{CDOM}}(\lambda) + a_{\text{NAP}}(\lambda). \tag{5}$$

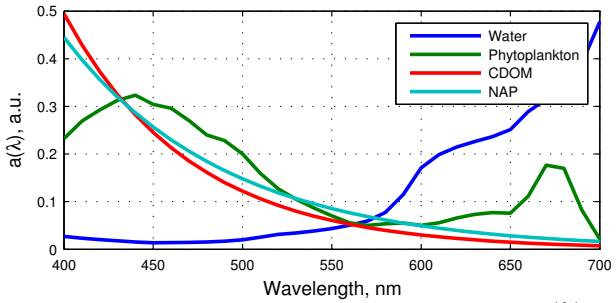

Figure 3: Shapes of the spectral absorption coefficient $a(\lambda)$ for different seawater constituents. Individual components are not shown to scale, y-axis represents arbitrary units.

Figure 3 shows the shapes of the spectral absorption coefficient of the four constituents. The absorption properties of each constituent has been extensively studied. The spectral absorption of pure seawater $a_w(\lambda)$ is fixed and well known [15, 16, 17]. The particular properties of phytoplankton and non-algal particles have both been shown to be related to the concentration of chlorophyll [18], while the absorption properties of the colored dissolved organic matter, also called yellow matter, are largely independent of the amount of chlorophyll [19, 10].

The CDOM spectral absorption is described well by a decaying exponential [19]

$$a_{\text{CDOM}}(\lambda) = a_{\text{CDOM},\lambda_0} e^{-0.014(\lambda-\lambda_0)}, \tag{6}$$

where λ_0, the reference wavelength, is often chosen to be 440nm, and $a_{\text{CDOM},\lambda_0}$ is the absorption at the reference wavelength. The scale in the exponent is experimentally determined and usually varies between -0.014 and -0.019 [19].

The absorption by non-algal particles (detritus) has a very similar form to that of CDOM [20]

$$a_{\text{NAP}}(\lambda) = a_{\text{NAP},\lambda_0} e^{-0.011(\lambda-\lambda_0)}, \tag{7}$$

with values of the scale in the exponent in the range of -0.006 to -0.014 [20]. Furthermore [18] showed that the detritus absorption at $\lambda_0 = 440$ is highly correlated to chlorophyll concentration C

$$a_{\text{NAP},440} = 0.0124 \cdot C^{0.724}. \tag{8}$$

Because of this correlation we are treating NAP absorption as a dependent variable fully specified by chlorophyll concentration C.

The spectral absorption of phytoplankton depends on its species as well as the concentration. The amount of phytoplankton is defined by the concentration of chlorphyll, one of its primary components. The spectral shape of the absorption curve is affected by the phytoplankton species, although the absorption curves for many phytoplankton species are similar with peak absorption around 450 and 650nm [21, 22]. The between-species similarities mean that phytoplankton absorption can be compactly represented with low-dimensional linear models

$$a_\Phi(\lambda) = \sum_{i=1}^{z} t_i(\lambda) w_i, \tag{9}$$

where $t_i(\lambda)$ are fixed phytoplankton absorption basis functions and w_i are the absorption basis weights. Furthermore [18] showed

DOI: 10.2352/ISSN.2470-1173.2016.18.DPMI-252

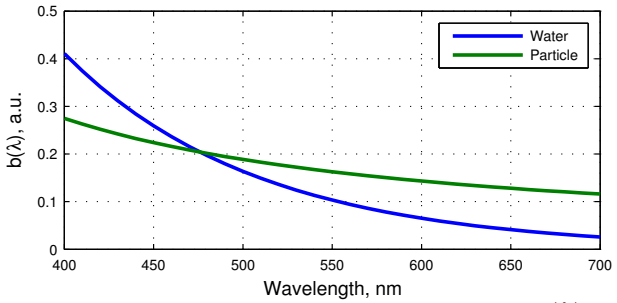

Figure 4: Shapes of the spectral scattering coefficient $b(\lambda)$ for different seawater constituents. Individual components are not shown to scale, y-axis represents arbitrary units.

that phytoplankton absorption is related to chlorophyl concentration C by

$$a_\Phi(440) = 0.0378 \cdot C^{0.627}. \tag{10}$$

A particular phytoplankton absorption spectrum can be generated by selecting a particular assignment of weights w that define the shape. Then the shape can be scaled, to satisfy (10).

Scattering coefficient

The total scattering coefficient $b(\lambda)$ can also be represented as a sum of the scattering coefficients of pure seawater $b_w(\lambda)$ and particulate matter components $b_p(\lambda)$

$$b(\lambda) = b_w(\lambda) + b_p(\lambda). \tag{11}$$

The spectral shapes for the two scattering components are presented in Fig. 4. As scattering depends much more on particle dimensions, rather than their biological origin, the constituents are divided according to their size into pico-, nano- and microparticles. Each particle class is modeled in the same way, even though it comprises phytoplankton, colored dissolved organic matter (CDOM) and non-algal particles (NAP).

Just as in the case of absorption, the scattering coefficient of seawater $b_w(\lambda)$ is fixed and known [16, 23]. The scattering coefficient of particulate matter $b_p(\lambda)$ depends on the concentrations of pico-, nano- and micropartciles. The concentrations of individual particle types types can be related to the total chlorophyll concentration C [24], and consequently express the total scattering coefficient as a function of a single parameter C

$$\begin{aligned} b_p(\lambda) = {} & b^\star_{p,1,2,\lambda_0} \left(\frac{\lambda}{\lambda_0}\right)^{-\gamma_{1,2}} \left[C_{1,2}\left(1 - e^{-S_{1,2}C}\right)\right] \\ & + b^\star_{p,3,\lambda_0} \left(\frac{\lambda}{\lambda_0}\right)^{-\gamma_3} \left[C - C_{1,2}\left(1 - e^{-S_{1,2}C}\right)\right] \\ & + b_{k,\lambda_0} \left(\frac{\lambda}{\lambda_0}\right)^{-\gamma_k}. \end{aligned} \tag{12}$$

In the above equation the subscript $1,2$ represents the contributions of pico- and nanoparticles, while the subscript 3 represents microparticles. Finally, a constant background contribution is given by b_k. The numerical values of experimentally determined model constants are summarized in Table 1

Table 1: Particle scattering coefficient model constants for $\lambda_0 =$ 470nm, data taken from [24].

Parameter	Unit	Value
$C_{1,2}$	mg m^{-3}	0.78
$S_{1,2}$	(mg)$^{-1}$ m^3	1.1449
$b^\star_{p,1,2,\lambda_0}$	m^2 mg^{-1}	0.0046
$b^\star_{p,3,\lambda_0}$	m^2 (mg)$^{-1}$	0.0005
b_{k,λ_0}	m^{-1}	0.00068
$\gamma_{1,2}$	–	0.7
γ_3	–	-0.2
γ_k	–	1.9

Discrete model

To simplify computation we discretize all spectral quantities to a small number, q, of narrow wavelength bands. The continuous wavelength representation of total attenuation

$$k(\lambda) = e^{-da(\lambda)}, \tag{13}$$

is replaced with a vector $k \in \mathbf{R}^q$, whose ith entry represents the total attenuation at wavelength λ_i

$$k_i = e^{-da(\lambda_i)}, \tag{14}$$

and where d is the distance traveled through the medium. To underline the dependence of the total attenuation k on model parameters $x = (w, C, a_{\text{CDOM},\lambda_0})^T$, the discretized attenuation is denoted $k(x)$.

Parameter estimation

The underwater image formation model can also be used to estimate model parameters from camera sensor data, such as the phytoplankton absorption spectrum, chlorophyl concentration and amount of colored dissolved organic matter, CDOM. Estimation involves finding a solution to a minimization problem

$$\underset{x,s}{\text{minimize}} \;\; \|M - P^T \mathbf{diag}(i)\mathbf{diag}(k(x))R - s\mathbf{1}^T\|_F^2 \tag{15}$$

$$\text{subject to } C \geq 0,\; a_{\text{CDOM},\lambda_0} \geq 0,\; Tw \geq 0 \tag{16}$$

$$(Tw)_{\lambda_0} = 0.0378 \cdot C^{0.627} \tag{17}$$

$$s \geq 0. \tag{18}$$

The matrix $M \in \mathbf{R}^{m\times n}$ represents sensor image pixel intensities of n different surfaces from a camera with m different spectral channels (for color consumer cameras $m = 3$). The columns of $P \in \mathbf{R}^{q\times m}$ are the spectral responsivity functions of the camera, quantized to q spectral bands, the vector $i \in \mathbf{R}^q$ is the spectral power distribution of the illuminant. The columns of matrix $R \in \mathbf{R}^{q\times n}$ contain n surface spectral reflectances, and the columns of matrix $T \in \mathbf{R}^{q\times z}$ contains z discrete plankton absorption basis functions. Finally the vector $s \in \mathbf{R}^m$ contains backscattered light estimates for each of the camera channels. These estimates are the same for all surfaces.

The minimization problem contains several constraints, all of which follow directly from the physical properties of the estimated quantities. Specifically, phytoplankton spectral absorption Tw, chlorophyll concentration C, CDOM reference absorption

©2016 Society for Imaging Science and Technology
DOI: 10.2352/ISSN.2470-1173.2016.18.DPMI-252

$a_{\mathrm{CDOM},\lambda_0}$ and scattering s are all non-negative quantities. Furthermore the phytoplankton spectral absorption curve, Tw, should be appropriately scaled (17), so that (10) holds.

The optimization problem (15) is not convex; it is difficult to solve for two reasons. First, the objective function, an l_2 norm of an exponential, is non-convex. Second, the equality constraint (17) is not linear. Since all functions that cause non-convexity are continuous, smooth and monotonic, we can use an iterative approach to solve the problem. First, at iteration t, we approximate the function $k(x)$ with its first order Taylor series expansion around an estimate x^t [6]. The same approach is used to approximate the the non-linear equality constraint (17). Next, we compute a solution of the now convex problem. Finally, we use the computed optimal parameter estimates as center points for Taylor series expansion at the next iteration. The process is repeated until no decrease in the objective is observed.

Experiments

We implemented the underwater image formation model in Matlab and used the Image Systems Engineering Toolbox [13] to simulate camera acquisition of a Macbeth test chart placed underwater. We used a model of a popular consumer camera with a Bayer RGB color filter array and a near infrared (NIR) filter. Convex optimization problems were solved using the `cvx` optimization toolbox [25]. We simulated different water types by varying the concentrations of chlorophyll C and the absorption of color dissolved organic matter CDOM, $a_{\mathrm{CDOM},\lambda_0}$. We chose $\lambda_0 = 440$nm as the reference wavelength for CDOM absorption estimates and we used phytoplankton basis functions derived from the data in [21]. This particular data set proved to be largely one-dimensional, and hence we chose a single basis function. Although the proposed algorithm can handle cases where phytoplankton absorption shape varies, in this simulation the shape of phytoplankton absorption was fixed and only the scale could vary. Finally, we generated tests scenes at different depths and target to camera distances.

Appearance simulation

We evaluate our model using qualitative comparisons between simulated target images and the images of a Macbeth chart submerged in different geographical locations. Figure 5 shows target appearance in clear waters of the Pacific Ocean in the proximity of Fanning Island. The blueish tint of the simulated test target was achieved by setting a low chlorophyll concentration $C = 1\mathrm{mg\ m^{-1}}$ and low CDOM absorption $a_{\mathrm{CDOM},440} = 0.05\mathrm{m}^{-1}$. Figure 6 presents a similar comparison for murky waters of the Monterey Bay, CA. To obtain a much stronger greenish tint of the target the chorophyll concentration was increased to $C = 5\mathrm{mg\ m^{-1}}$ and CDOM absorption was set to $a_{\mathrm{CDOM},440} = 0.1\mathrm{m}^{-1}$.

Figure 7 further explores the changes in the appearance of the test target when different model parameters are selected. Specifically color appearance changes are much more pronounced with increasing target depth (Fig. 7, top row). As light travels deeper underwater, it is attenuated more and more strongly and the colors become less and less pronounced. Changes in the camera to target distance (Fig. 7, bottom row) have a much smaller effect on the overall color appearance.

Figure 8 shows the appearance changes as the function of chlorophyll concentration. The concentration was adjusted between $C = 0.01\mathrm{mg\ m^{-1}}$ (open ocean waters) and $C = 100\mathrm{mg\ m^{-1}}$ (eutropic estuaries, lakes) [10]. As expected the overall hue changes from blueish, characteristic of pure water absorption, to greenish, where absorption is dominated by phytoplankton.

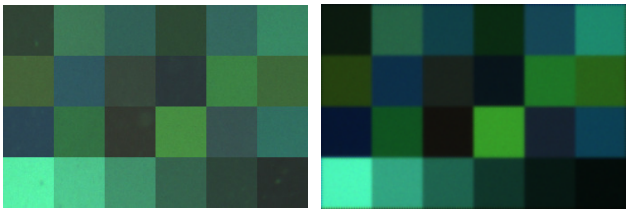

(a) Captured (b) Simulated

Figure 5: Target appearance in clear water conditions (Fanning Island, Pacific Ocean). Images are not gamma encoded.

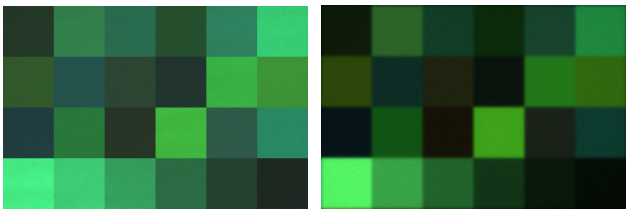

(a) Captured (b) Simulated

Figure 6: Target appearance in murky water conditions (Monterey Bay, CA). Images are not gamma encoded.

Parameter estimation

The estimation algorithm finds model parameters $x = (w, C, a_{\mathrm{CDOM},\lambda_0})^T$ so that the resulting light attenuation $k(x)$ produces the best fit between the image formation model and the measured or simulated data M. Figure 9 compares a sample attenuation estimate $k(x)$ to the ground truth data for a particular set of medium properties and scene geometry.

The high quality of the estimate does not depend on the specific medium characteristics. Figure 10 plots the relative root-mean-squared error (RRMSE) defined as

$$\mathrm{RRMSE} = \frac{\|\hat{y} - y\|}{\sqrt{q}\|y\|}, \tag{19}$$

where $y, \hat{y} \in \mathbf{R}^q$ represent the true and estimated quantity respectively. The RRMSE values are computed for different depths and camera to scene distances and averaged across different chlorophyll concentrations and CDOM absorption values. Note that this relative error remains small, about 2%, but increases slightly with larger depths and target distances.

The wavelength dependence of the spectral attenuation $k(\lambda)$ predicts the color of water. As the light travels deeper into the medium, its spectral composition, and thus colors, are affected. The information about the shape of spectral absorption curve can be used to correct the colors of underwater images. Figure 11, left, represents the appearance of the underwater target used to derive the attenuation curve . This attenuation curve was then used to estimate the effective ambient illuminant and to calculate the coefficients in a diagonal (von Kries, [26]) illuminant correction (see Fig 11, right). The attenuation curve in Fig. 9 was derived from the top left image in Fig. 11.

Although the algorithm can predict spectral attenuation with high accuracy, the inverse estimation algorithm may be ill-posed

DOI: 10.2352/ISSN.2470-1173.2016.18.DPMI-252

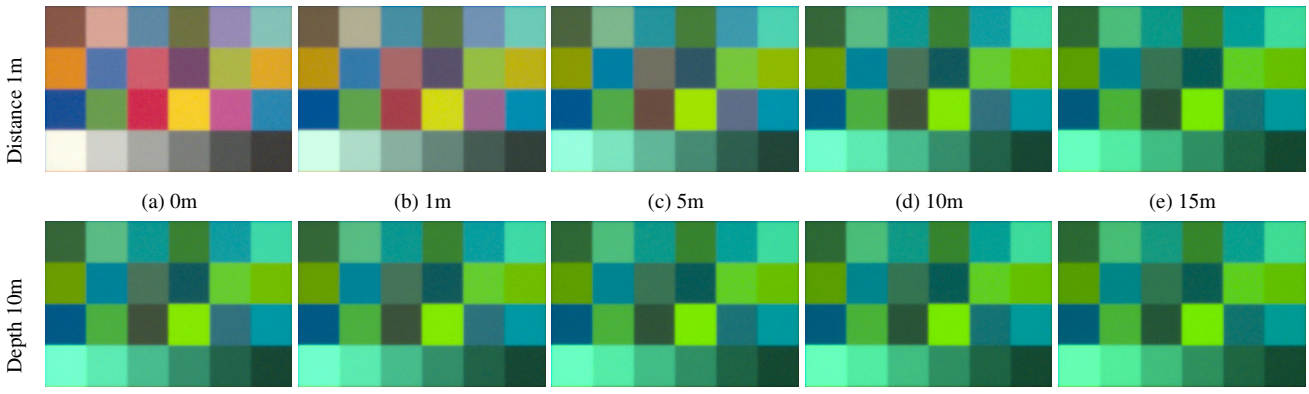

(a) 0m (b) 1m (c) 5m (d) 10m (e) 15m

(f) 1m (g) 2m (h) 5m (i) 7m (j) 10m

Figure 7: Macbeth test target appearance for different scene geometries: targed distance and depth with fixed seawater properties: $a_{\mathrm{CDOM},440} = 0.1\mathrm{m}^{-1}$, $C = 1\mathrm{mg\ m}^{-3}$.

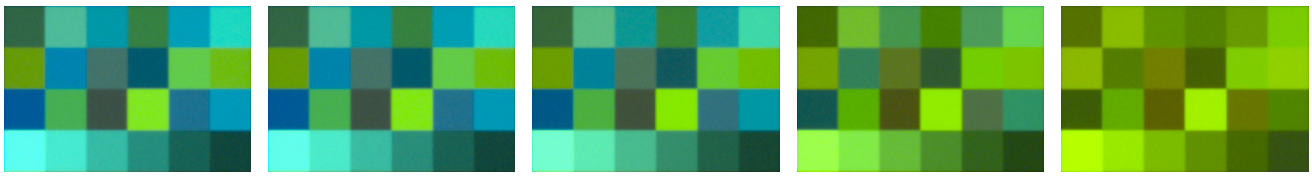

(a) 0.01mg m^{-3} (b) 0.1mg m^{-3} (c) 1mg m^{-3} (d) 10mg m^{-3} (e) 100mg m^{-3}

Figure 8: Macbeth test target appearance for different chlorophyll concentrations. The target is submerged to 10m and is 1m away from the camera, CDOM absorption is fixed: $a_{\mathrm{CDOM},440} = 0.1\mathrm{m}^{-1}$.

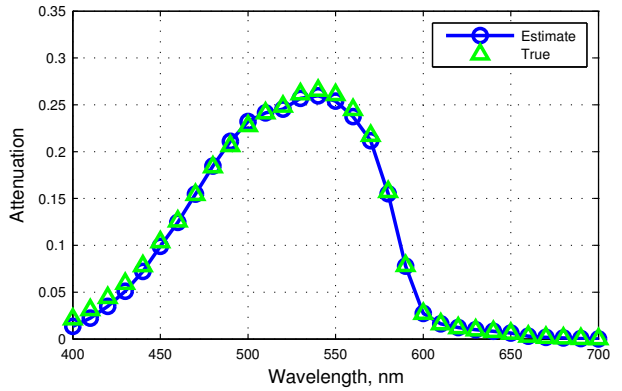

Figure 9: Light attenuation estimation example, depth 10m, distance 5m, $C = 1\mathrm{mg\ m}^{-3}$ and $a_{\mathrm{CDOM},440} = 0.1\mathrm{m}^{-1}$.

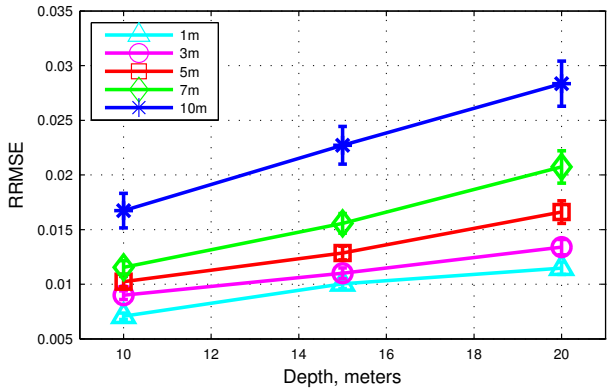

Figure 10: Errors in light attenuation estimation. Each point represents the average RRMSE and the corresponding standard error across different phytoplankton concentrations C and CDOM absoprtions $a_{\mathrm{CDOM},440}$.

when it comes to predicting the model parameters for phytoplankton concentration and CDOM. Different numerical values of these model parameters can produce the same spectral attenuation curves. It is, therefore, interesting to compare the estimated and ground truth values for the amount of phytoplankton and CDOM in sea water at different depths and for different target distances. Figure 12 shows that the difference between true and estimated parameter values for both phytoplankton and CDOM concentration is relatively small at small depths and increases with water depth. Across different conditions Pearson's correlation coefficient between the true and estimated quantities is consistently above 0.7.

Similar analysis, presenting the correlation between true and estimated colored dissolved organic matter (CDOM) absorption $a_{\mathrm{CDOM},440}$, is shown in Fig. 13. Again, parameter estimates be-

©2016 Society for Imaging Science and Technology
DOI: 10.2352/ISSN.2470-1173.2016.18.DPMI-252

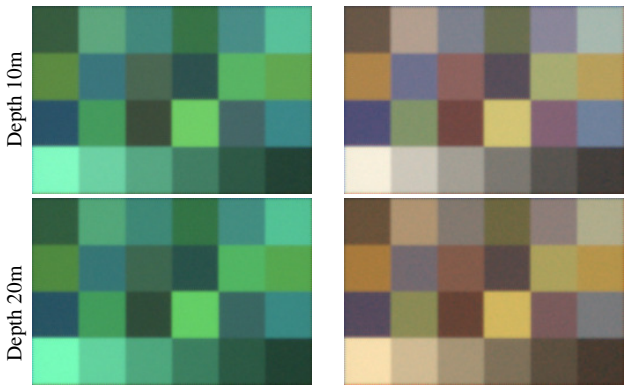

(a) (b)

Figure 11: Color correction of underwater image at a fixed distance of 5m. The original image (a) was used to estimate the absorption which provided the von Kires model coefficients for illuminant correction (b). The intensities of images at the two depths are similar because the two images have been normalized.

come less accurate with an increase in depth as well as chlorophyll concentration.

Although the accuracy in predicting the parameter values for phytoplankton and CDOM concentration decreases with increasing depth and target distance, we can still use the estimated total light attenuation as a good model for the ambient illumination. In other words, analysis of the underwater images we capture of objects that are far away from the camera and deep in the ocean may not yield good estimates for the amount of phytoplankton and CDOM, they do nonetheless give us a useful estimate of the ambient illumination that can be used for color correction (Fig. 12).

Conclusions

We presented an underwater image formation model connecting underwater scene appearance with biologically meaningful quantities such as chlorophyll concentration, plankton species and the amount of color-dissolved organic matter (CDOM). By adjusting a small number of parameters we were able to reproduce images of underwater targets captured in different areas of the world and in different water conditions.

Next, we proposed an inverse estimation algorithm that uses an image of a known target captured with a simple camera to estimate the total light attenuation spectrum due to water and its constituents. We showed that the derived attenuation spectrum could be used to color balance underwater images.

Finally, we investigated the use of conventional consumer color cameras as scientific measurement devices. In addition to the spectral attenuation curve, our estimation algorithm can derive estimates for biologically relevant water constituents such as the amount of phytoplankton and color dissolved matter (CDOM) in the water. Our simulations show that there is a high correlation between the estimates and the ground truth parameters, particularly when the water depth is less than 10 meters.

We are now extending this work by modeling consumer digital cameras with attached lighting to explore how we can improve our estimates at deeper water depths. And we are using the same methodology (simulation and estimation) to study the health of coral reefs [27].

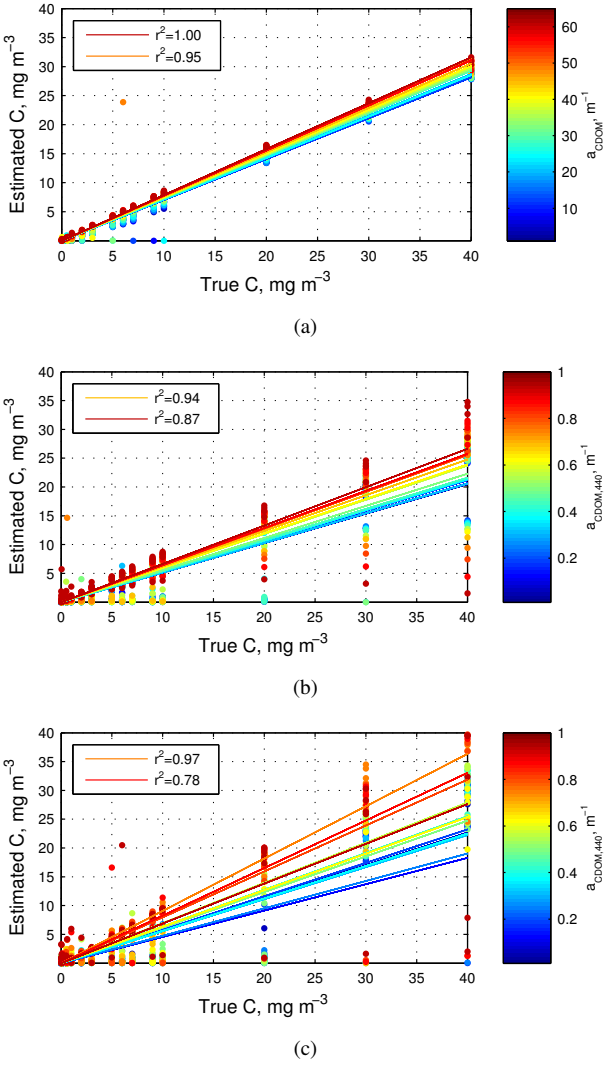

Figure 12: Chlorophyll concentration estimation accuracy for a fixed scene to target distance of 1m, different depths: (a) 5m, (b) 10m, (c) 20m and different values of $a_{\text{CDOM},440}$. Different colors correspond to different values of CDOM absorption $a_{\text{CDOM},440}$. Pearson's correlation coefficient r^2 varies between 1 and 0.7 and decreases with an increase in depth and lower CDOM absorption values.

DOI: 10.2352/ISSN.2470-1173.2016.18.DPMI-252

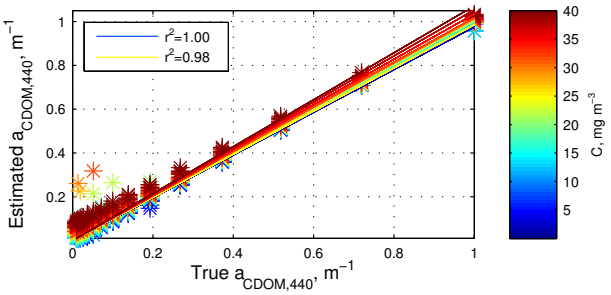

(a)

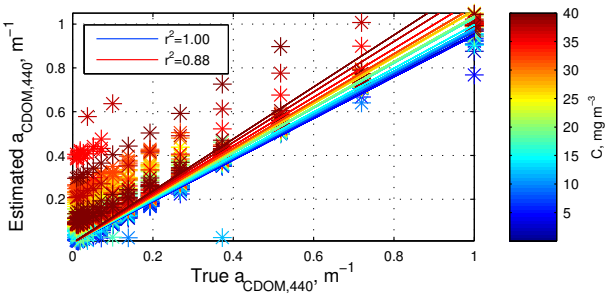

(b)

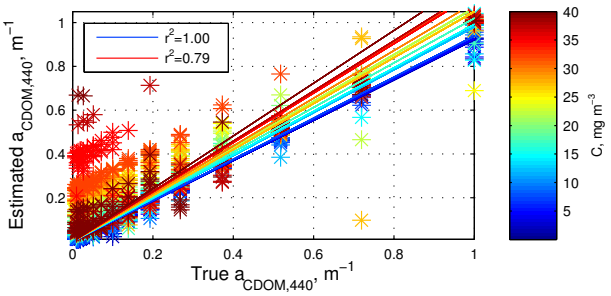

(c)

Figure 13: Colored dissolved organic matter absorption $a_{\mathrm{CDOM},440}$ estimation accuracy for a fixed scene to target distance of 1m, different depths: (a) 5m, (b) 10m, (c) 20m and different values of phytoplankton concentration C. Color coding represents different values of C. Pearson's correlation coefficient r^2 varies between 1 and 0.7. Estimate accuracy decreases with increasing depth and chlorophyll concentration.

References

[1] M. Boffety, F. Galland, and A.-G. Allais, "Color image simulation for underwater optics," *Applied optics*, vol. 51, no. 23, pp. 5633–5642, 2012.

[2] A. Sedlazeck and R. Koch, "Simulating Deep Sea Underwater Images Using Physical Models for Light Attenuation, Scattering, and Refraction," in *Vision, Modeling, and Visualization*, P. Eisert, J. Hornegger, and K. Polthier, Eds. The Eurographics Association, 2011.

[3] J. Y. Chiang and Y.-C. Chen, "Underwater image enhancement by wavelength compensation and dehazing," *IEEE Transactions on Image Processing*, vol. 21, no. 4, pp. 1756–1769, 2012.

[4] R. Schettini and S. Corchs, "Underwater image processing: state of the art of restoration and image enhancement methods," *EURASIP Journal on Advances in Signal Processing*, vol. 2010, p. 14, 2010.

[5] J. Åhlén, D. Sundgren, and E. Bengtsson, "Application of underwater hyperspectral data for color correction purposes," *Pattern Recognition and Image Analysis*, vol. 17, no. 1, pp. 170–173, 2007.

[6] H. Blasinski, J. Breneman, and J. Farrell, "A model for estimating spectral properties of water from RGB images," in *IEEE International Conference on Image Processing ICIP*, Oct 2014, pp. 610–614.

[7] J. Breneman, H. Blasinski, and J. Farrell, "The color of water: using underwater photography to assess water quality," in *IS&T/SPIE Electronic Imaging*. International Society for Optics and Photonics, 2014, pp. 90 230R–90 230R.

[8] Z. Lee, K. L. Carder, and R. A. Arnone, "Deriving inherent optical properties from water color: a multiband quasi-analytical algorithm for optically deep waters," *Applied Optics*, vol. 41, no. 27, pp. 5755–5772, Sep 2002.

[9] X. Zhao, T. Jin, and S. Qu, "Deriving inherent optical properties from background color and underwater image enhancement," *Ocean Engineering*, vol. 94, pp. 163–172, 2015.

[10] C. Mobley, *Light and water: Radiative transfer in natural waters*. Academic Press, 1994.

[11] J. Jaffe, "Computer modeling and the design of optimal underwater imaging systems," *IEEE Journal of Oceanic Engineering*, vol. 15, no. 2, pp. 101–111, 1990.

[12] B. McGlamery, "A computer model for underwater camera systems," in *Ocean Optics VI*. International Society for Optics and Photonics, 1980, pp. 221–231.

[13] J. E. Farrell, P. B. Catrysse, and B. A. Wandell, "Digital camera simulation," *Applied Optics*, vol. 51, pp. A80–A90, 2012.

[14] B. Wandell, *Foundations of vision*. Sinauer Associates, 1995.

[15] H. Buiteveld, J. Hakvoort, and M. Donze, "Optical properties of pure water," in *Ocean Optics XII*. International Society for Optics and Photonics, 1994, pp. 174–183.

[16] R. Smith and K. Baker, "Optical properties of the clearest natural waters (200–800nm)," *Applied optics*, vol. 20, no. 2, pp. 177–184, 1981.

[17] S. Sullivan, "Experimental study of the absorption in distilled water, artificial sea water, and heavy water in the visible region of the spectrum," *Journal of the Optical Society of America*, vol. 53, no. 8, pp. 962–967, 1963.

[18] A. Bricaud, A. Morel, M. Babin, K. Allali, and H. Claustre, "Variations of light absorption by suspended particles with chlorophyll a concentration in oceanic (case 1) waters: Analysis and implications for bio-optical models," *Journal of Geophysical Research: Oceans*, vol. 103, no. C13, pp. 31 033–31 044, 1998.

DOI: 10.2352/ISSN.2470-1173.2016.18.DPMI-252

[19] A. Bricaud, A. Morel, and L. Prieur, "Absorption by dissolved organic matter of the sea (yellow substance) in the UV and visible domains," *Limnology Oceanogr*, vol. 26, no. 1, pp. 43–53, 1981.

[20] C. Roesler, M. Perry, and K. Carder, "Modeling in situ phytoplankton absorption from total absorption spectra in productive inland marine waters," *Limnology and Oceanography*, vol. 34, no. 8, pp. 1510–1523, 1989.

[21] T. Fujiki and S. Taguchi, "Variability in chlorophyll-a specific absorption coefficient in marine phytoplankton as a function of cell size and irradiance," *Journal of Plankton Research*, vol. 24, no. 9, pp. 859–874, 2002.

[22] S. Sathyendranath, L. Lazzara, and L. Prieur, "Variations in the spectral values of specific absorption of phytoplankton," *Limnology and Oceanography*, vol. 32, no. 2, pp. 403–415, 1987.

[23] A. Morel, "Optical properties of pure water and pure sea water," *Optical aspects of oceanography*, vol. 1, pp. 1–24, 1974.

[24] R. Brewin, G. DallOlmo, S. Sathyendranath, and N. Hardman-Mountford, "Particle backscattering as a function of chlorophyll and phytoplankton size structure in the open-ocean," *Optics express*, vol. 20, no. 16, pp. 17 632–17 652, 2012.

[25] M. Grant and S. Boyd, "CVX: Matlab software for disciplined convex programming, version 2.1," http://cvxr.com/cvx, Mar. 2014.

[26] J. von Kries, "Die gesichtsempfindungen," *Handbuch der physiologie des menschen*, vol. 3, pp. 109–282, 1905.

[27] H. Blasinski and J. Farrell, "Simulation of underwater imaging systems," in *Imaging Systems and Applications*. Optical Society of America, 2015, pp. IT3A–3.

Author Biography

Henryk Blasinski received the M.S. degree (Hons.) in telecommunications and computer science from the Lodz University of Technology, Lodz, Poland, and the Diplome d'Ingeneiur degree from the Institut Superieur dElectronique de Paris, France, in 2008 and 2009, respectively. He was a Fulbright Scholar with the Department of Electrical and Computer Engineering, University of Rochester, Rochester, NY, from 2010 to 2011. At present he is pursuing a Ph.D. degree at the Department of Electrical Engineering, Stanford University, CA. Henryk's research interests include image processing, human and computer vision and machine learning.

Joyce Farrell is the Executive Director of the Stanford Center for Image Systems Engineering and a senior research associate in the Department of Electrical Engineering at Stanford University. She has a doctorate degree from Stanford University and more than 20 years of research and professional experience working at a variety of companies and institutions, including the NASA Ames Research Center, New York University, the Xerox Palo Alto Research Center, Hewlett Packard Laboratories and Shutterfly.